3D-Ballistocardiography in microgravity: comparison with ground based recordings

P-F. Migeotte, *Member, IEEE*, Quentin Delière, J. Tank, I. Funtova, R. Baevsky, X. Neyt, *Member, IEEE*, N. Pattyn

***Abstract*—3D-Ballistocardiograms ECG and Impedance-cardiograms (ICG) were recorded on 5 healthy volunteers participating to the European Space Agency (ESA) 57th parabolic flights campaigns. Comparisons are made between the baseline recordings performed on the ground and the recordings made during the microgravity phases of a parabolic flight. The spatial curves of the displacement, velocity and acceleration vectors, instead of their individual components are used to compute the magnitude of the force vector, kinetic energy and work during the cardiac cycle. Our hypothesis is that the 3D-BCG provides parameters correlated with the timings of ejection (PEP, LVET). Although our subject population is limited (N=5), this is the first study of BCG to be performed with N>1. Our results suggest that microgravity decrease the complexity of the 3D displacement curve and that peaks in curvature are consistently present in microgravity and on the ground. However they do not seem to be perfectly related to the classical cardiac ejection timings from ICG.**

I. Introduction

BALLISTOCARDIOGRAPHY, in the lab, is typically studied on subjects lying on a table, sitting on a chair, or standing on a scale where forces, accelerations, velocities or displacements originating from cardiac activity are recorded. In the vast majority of cases, the research is limited to 1D or 2D analysis of the ballistocardiogram (BCG) components in the frontal plane. Most of the physiological interpretations are drawn from the component along the longitudinal (foot-to-head) axis. Since the early days of the Ballistocardiography, attempts were made to record a vecto-ballistocardiogram, i.e. a recording of the accelerations or forces in the 3-dimensions (3-D) of space [5]. Moreover the influence of gravity along one of the measurement axis implies that large differences between standing and supine recordings that are due to the intrinsic anisotropic conditions. Hence since the beginning of the space exploration era attempts to record 3D-BCG in microgravity were made [1,2,3]. In previous work [3,4] we reported results from a data set of 3-D BCG which was recorded in 1993 on a crew member of the Spacelab-D2 mission. In the present paper we apply the same methodology to recordings performed in the transient microgravity environment obtained during parabolic flights. We compare the 3D displacement curves, and their geometrical characteristics invariants, such as peaks in curvature and torsion, obtained on the same subject in free-float to the baseline recordings performed on the ground in standing and supine positions. Our results were obtained during the ESA 57th parabolic flight campaigns conducted on-board the A300-zéroG airplane of NOVESPACE.

While our limited number of subject and the inhomogeneity of our sample population (2 female, 3 male) does not allow yet proper statistics, the preliminary results are encouraging and the statistics will be soon improved with our participation to the next parabolic flight campaign (april-mai 2013).

Our hypothesis is that the 3D-BCG provides parameters correlated with the timings of ejection, i.e. pre ejection period (PEP) and left ventricular ejection time (LVET). Moreover we expect that microgravity allows recording of 3D-BCG curve with more stable conditions and that the symmetrical nature of the curve will be more preserved than during the ground based recordings.

II. Protocols and Experimental Procedures

The technical details are described more extensively in previous work [3, 4, 6].

A. Experimental procedure

3-D accelerations, ECG, Impedance cardiogram (ICG) and respiration signal (nasal thermistor) were recorded, at 1kHz using a modified PNEUMOCARD system [4]. Data was recorded on 5 healthy subjects on the ground (~60 s standing and supine) and while free-floating during the ~20s of microgravity phases of the parabolic maneuver of the A300-ZéroG airplane of NOVESPACE. Sensor was placed close to the center of mass (CM) of the subject in order to provide a 3D-BCG.

B. Subjects & protocols

Data were recorded on five healthy subjects: two women and three men, age 35 ± 12 years, weight 70 ± 15 kg, height 176 ± 14 cm. The protocols were noninvasive, reviewed and approved by the local institutional ethical review boards and the pertinent French authorities. Informed consent of the subjects were obtained after the inclusion visit.

Manuscript received February 06, 2013. This work was supported by the Belgian Federal Science Policy Office (BELSPO) via the European Space Agency PRODEX program. P-F. Migeotte, X. Neyt, N. Pattyn and Q. Delière are with the Vital Signs and Performance research unit of the Royal Military Academy, Brussels, Belgium (email: pfmigeot@elec.rma.ac.be). Tank is with the Institut für Klinische Pharmakologie, Medizinische Hochschule Hannover, Germany. R Baevsky and I. Funtova are with the Laboratory for autonomic regulation of cardiorespiratory system, Institute of Biomedical problems, Moscow, Russian academy of sciences, Russian Federation.

C. Axis System

We chose to use the nomenclature for the axes that is the standard in ballistocardiography, where *x* is the lateral (left-to-right) axis, *y* is the longitudinal body (foot-to-head) axis, and *z* is the antero-posterior (ventro-dorsal) axis.

III. Methods

A. Ensemble averaging, Drift removal & Integration

R waves of the ECG were automatically identified, visually inspected, and edited if required. For each cycle (from R to R wave), the ECG and BCG data were sliced, and time aligned: time axis was normalized so that the beginning of each cycle was set to 0 and the end to 1000. ECG and BCG curves from different heart-beats were superimposed and ensemble averaged. This allows taking into account the normal heart rate variability. A low pass filtering procedure was applied to remove all components of a lower frequency than the instantaneous heart rate of the subject [3, 4]. This includes removal of drift and components due to respiration. Acceleration components are then integrated to provide the corresponding 3D velocity and 3D displacement components.

Figure 1 present the displacement curve in the 3 anatomical projections. To facilitate the physiological interpretation the coordinate of displacement were inverted in order to represent the displacement of the moving parts (predominately blood) during one cardiac cycle. A color coding was used to represent different time intervals within the cardiac cycle (Fig. 1).

B. Characterization of the 3-D curve

We used the Frenet-Serret relationship of vector differential analysis to characterize the curve with scalar parameters independent of the frame of reference. Let

$$\vec{r} = x\hat{i} + y\hat{j} + z\hat{k} \qquad (1)$$

describes the location of the point (*x*,*y*,*z*) in the coordinates $(\hat{i}, \hat{j}, \hat{k})$. $d\vec{r}$ is the vector of infinitesimal changes *dx*, *dy*, *dz*. The infinitesimal distance, *ds*, between two nearby points is given by:

$$ds = \sqrt{dx^2 + dy^2 + dz^2} \qquad (2)$$

Using the dot notation for derivative over time, $\dot{r}$ and $\ddot{r}$ denotes the velocity and acceleration vectors, respectively. The curve can be further characterized by its curvature

$$\frac{1}{\rho^2} = \frac{\left|\dot{r} \times \ddot{r}\right|}{\mathrm{ds}^6} \qquad (3)$$

and its torsion

$$\frac{1}{\tau} = \frac{\left|\dot{r} \cdot \ddot{r} \cdot \dddot{r}\right|}{\left|\dot{r} \times \ddot{r}\right|^2} \qquad (4)$$

where ρ and τ are the radius of curvature and torsion. These parameters are presented in Fig.1.

Singular value decomposition (SVD) of the displacement curve was used to identify the curve plane of symmetry (see more details in [3]). The amount of excursion outside that plane will be denoted as w3.

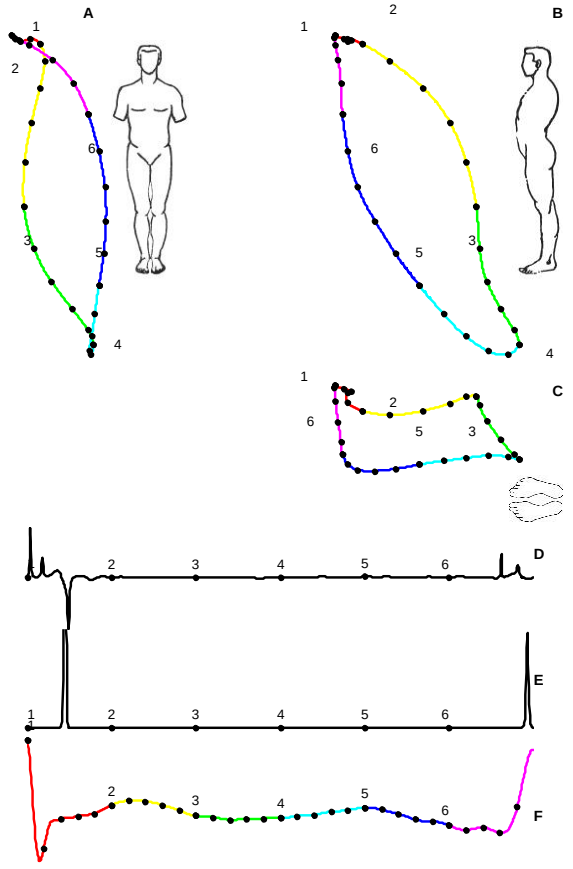

Fig. 1. Projections of the displacement on the 3 anatomical planes: (A) frontal, (B) sagittal, and (C) transverse. Torsion (D), curvature (E) and the ECG (F) presents numerical labels for time axis identification. ECG is color coded to represent regular time intervals. Displacements coordinates were inverted so that the loop represents the movement of moving elements within the body (mostly blood). Data from a free-floating subject in parabolic flight.

Figure 2 presents the same curve as in Fig. 1 after SVD decomposition, and reconstruction after nulling the third component (w3). Note that a second peak in curvature appears in the systolic phase. Due to a large difference in amplitude, the peak is not visible in Fig.1 however it was also present in the curvature data.

C. Acceleration vector,

Figure 3 presents the longitudinal component of BCG (BCG-y-axis) together with the magnitude of the force vector computed as:

$$\left|\vec{F}\right| = m \cdot \sqrt{a_x^2 + a_y^2 + a_z^2} \qquad (5)$$

where m is the mass of the subject.

D. Velocity and Kinetic Energy

Components of velocity are computed as the integral of the acceleration components and kinetic energy is given by:

$$K = \frac{1}{2} m \cdot \sqrt{v_x^2 + v_y^2 + v_z^2} \quad (6)$$

Kinetic energy of the same data set of Fig.1 is presented in Fig. 3 with the ECG, magnitude of Force and Work. It is seen that K present a large peak just after the main peak in

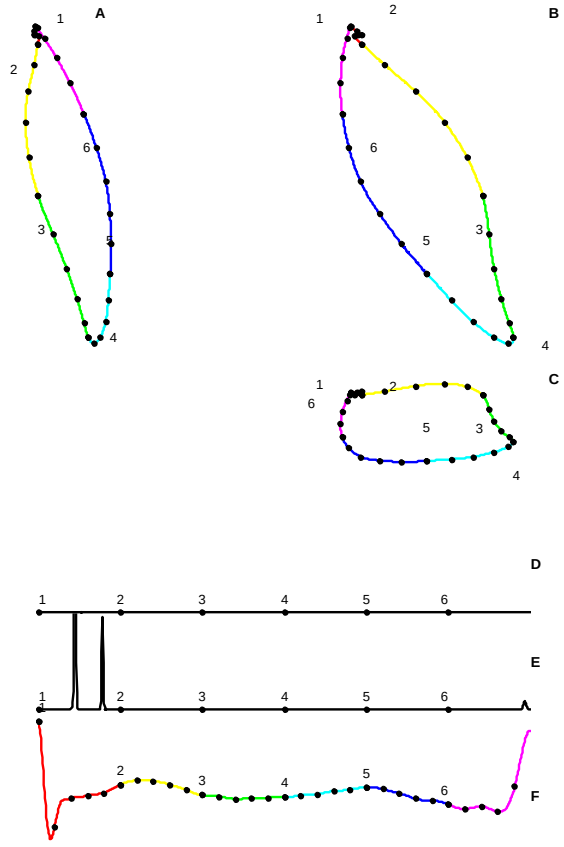

Fig. 2. Projections of the displacement curve reconstructed via SVD after nulling the third spatial component (same data set as in Fig.1). Projections on the 3 anatomical planes: (A) frontal, (B) sagittal, and (C) transverse. Torsion (D), curvature (E) and the ECG (F) Labels and time color coding as in Fig.1. Note that torsion vanishes.

the magnitude of the force vector. K present a second phase of increase during the late diastolic phase. This might be linked to the return of blood to the right heart.

E. Work

Components of displacement are computed as the integral of the velocity components and Work is given by:

$$dw = d\vec{F} \cdot d\vec{r} \quad (7)$$

where $d\vec{F}$ denotes the increment of force and $d\vec{r}$ is the increment of the vector position. Work presents maxima when Kin is low and/or when either the force or the displacement vector present large values.

F. Timings and parameters

From the timings of events in the signals (ECG, ICG and BCG-y component) as well as from computed values of Force, displacement, Kinetic Energy, Work and curvature, the following parameters were determined on ensemble averaged curve for each subject and posture condition: pre-ejection period (PEP); left ventricular ejection time (LVET); amplitude of ICG C-wave; time interval of R-peak to the main curvature peak preceding ejection phase (R-C1) as assumed the first peak before Fmax; time interval between C1 and C2 the main peaks in curvature surrounding ejection phase (C1-C2) as assumed to be first peak before and after Fmax; time interval from R to F max, K max and Work max, respectively; amount of excursion outside the plane of symmetry (w3); total displacement length within the cardiac cycle;

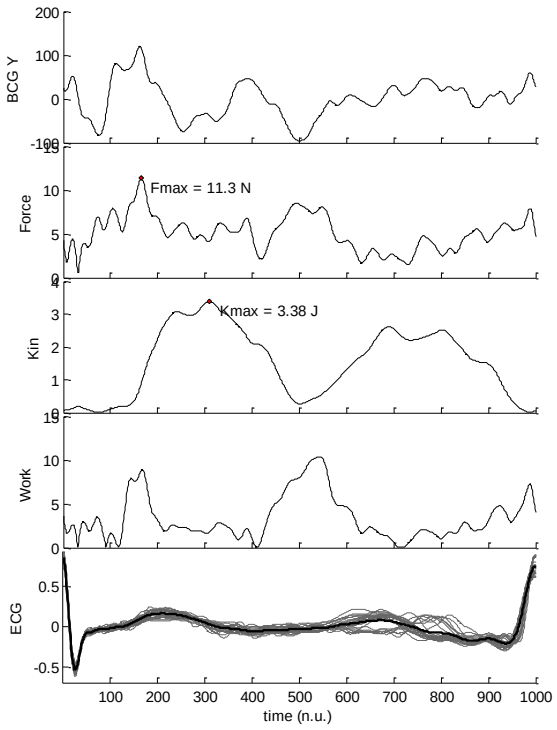

Fig. 3. From top to bottom: Longitudinal component of BCG (y-axis); magnitude of Force (N); Kinetic energy (10^{-3} J); Work (10^{-4}J); beat-by-beat ECG; Ejection is followed by a succession of peaks starting with Force Kinetic Energy (Kin) and Work which presents peaks in opposite phase of Kin.

IV. Results & Discussion

Timings and parameters were computed for each subject and each condition (supine, standing and free-floating) on a selection of heart beats which was performed to exclude artifact data coming from unavoidable collisions of the subject with the airplane walls. There are important limitations to our study: the number of subject is limited and our population is rather inhomogeneous. Moreover only 224 heart beats, i.e. 5,6 % of the total number of heart beats recorded in microgravity, could be analyzed. Therefore we can hardly expect significant results from statistical comparison.

Figure 4 presents the results from the reference parameters: RRI, amplitude of the ICG C wave which should present variations correlated to stroke volume (SV), PEP, RC1 which is the time delay between the R-wave (contraction of the ventricle) and the main peak in curvature

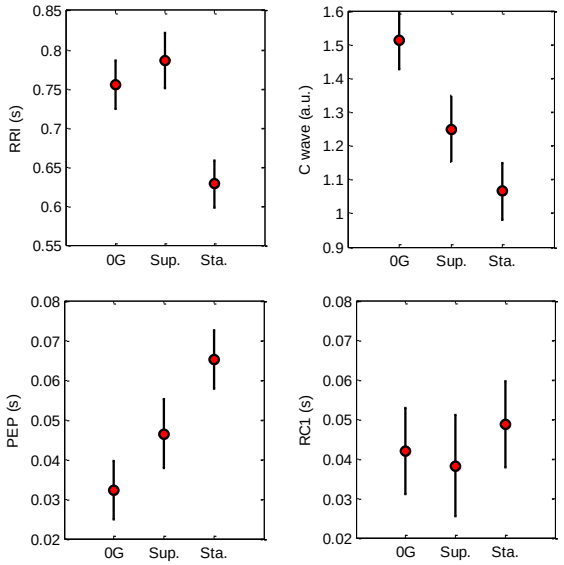

Fig. 4. From top to bottom and left to right: Mean ± SEM of RRI; ICG-C-wave amplitude; PEP (s) and timing of R-wave to first peak in curvature (RC1). Microgravity (0G) and Standing (sta.) N=5; Supine (Sup.) N=4.

preceding the peak in Force which is supposed to be linked to the ejection of blood in the aorta. The largest C-wave amplitude, larger RRI in 0G compared to standing and shorter PEP are the expected response in transient microgravity [7] and the first two are the only differences that are significant ($p<0.05$). RC1 presents a very stable behavior which, compared to the observed changes in PEP, suggests that the peak in curvature is probably more related to the mechanical contraction and recoil of the heart than to the opening of the aortic valve.

Figure 5 presents values of LVET and C1-C2, the timing

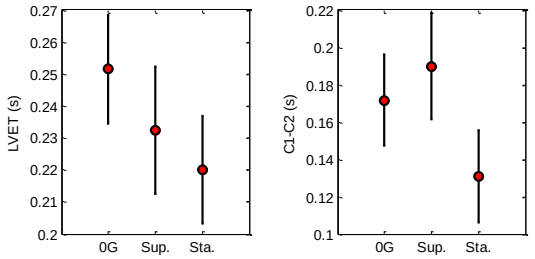

Fig. 5. From left to right: Mean ± SEM of LVET; timing of first peak in curvature (C1) to the second peak in curvature (C2). Microgravity (0G) and Standing (sta.) N=5; Supine (Sup.) N=4.

between the two main peaks in curvature that surrounds the ejection phase marked by the largest peak in Force magnitude. Our hypothesis was that both peaks in curvature could be linked to the opening and closure of the aortic valve thus RC1 should present the same behavior as PEP and C1-C2 should present the same changes as LVET. Our results suggests here that we should reject this hypothesis and that the peaks in curvature are probably linked to other aspects of the cardiac contraction.

Figure 6 presents results of Fmax, K max and Work max.

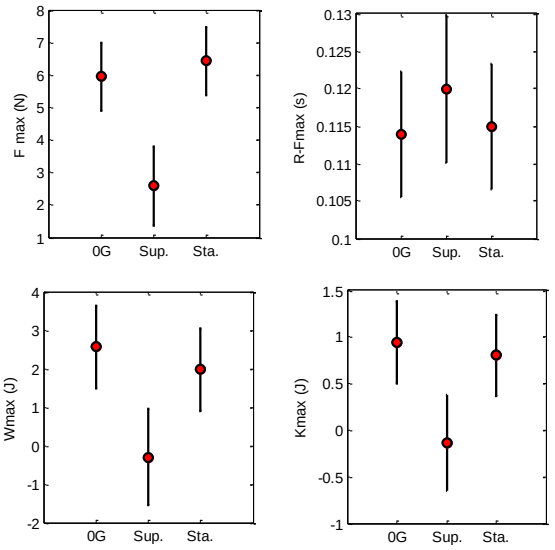

Fig. 6. From top to bottom and left to right: Mean ± SEM of F max; R-Fmax timing (s); Wmax (J); Kmax (J). Microgravity (0G) and Standing (sta.) N=5; Supine (Sup.) N=4.

The three parameters show very similar changes from microgravity (0G) to supine and standing while timing from R to Fmax does not show similarity with changes in PEP or RRI. Thus this suggests that the timing of Fmax is, as for C1 and C2, also probably not perfectly linked to the ejection timings. However we cannot exclude that our interpretation is influenced by the limited amount of data available and the limitations of the study that we presented beforehand.

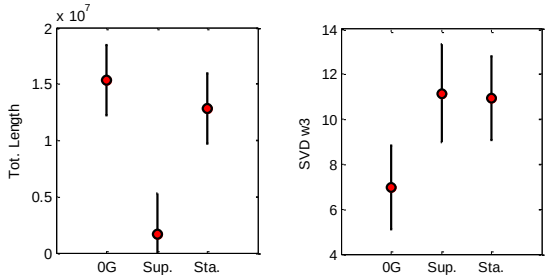

Fig. 7. From left to right: Mean ± SEM of LVET; Total 3D curve length within the cardiac cycle, SVD w3, the weight of the disregarded spatial component in the SVD reconstruction. Microgravity (0G) and Standing (sta.) N=5; Supine (Sup.) N=4.

Figure 7 presents the total length of the curve during one cardiac cycle and the weight of the third component of the SVD (w3) that is disregarded for the reconstruction of displacement in its plane of symmetry. The very small values seen in supine on the ground are probably linked to the specific conditions of our experiment: the subject was lying on his back with the accelerometer sensor placed in his back, thus in between the subject and the matrass on which he was lying. The smaller value seen in microgravity for w3 suggests that the curve is more symmetrical in microgravity than on the ground. This is likely linked to the absence of gravity influence which allows isotropic recording conditions. It is remarkable to see that the length of the curve

presents also similar changes as for Fmax, Kmax and Wmax.

V. Conclusion

Although the small N of our study does not allow sufficient power to allow consistent statistical analysis, this is the first study of BCG in microgravity performed in more than one subject. Parabolic flight experiments are tremendously difficult to conduct and we gathered only ~5% of artifact free data. However the observed changes in parameters and timings extracted from the reference method of ICG, shows the expected changes associated with microgravity. Furthermore while individual 3D curves were of a very variable shape, our results from the 3D-BCG analysis suggests that consistent peaks in the curvature signal are observed whether the subject is supine, standing or in free-float. They seem to be associated more to the cardiac contraction than to the ejection phase which is opposite to our initial hypothesis. We also observed that in microgravity the complexity of the 3D curve was decreased in a way that the displacement presents less excursions outside its plane of symmetry, thus supporting our hypothesis of a more stable and less disturbed 3D-BCG curve than on the ground with the influence of gravity.

Acknowledgment

We thank the participants to the parabolic flights and we acknowledge the perfect support from ESA and NOVESPACE for the organization of the parabolic flights campaign.

References

[1] Baevskii RM, Chattardzhi PS, Funtov II and Zakatov MD. Contractile function of the heart during weightlessness according to the results of 3-dimensional ballistocardiography. *Kosm. Biol. Aviakosm. Med*. 21: 26-31, 1987.

[2] Hixson, W.C., Dietrich, E.B., "Biotelemetry of the Triaxial Ballistocardiogram and Electrocardiogram in a Weightless Environment", U.S. Naval Medical Center, Pensacola, *Monograph 10*, N66-16283

[3] Prisk GK., Verhaeghe, S. Padeken, D., Hamacher H., Paiva.M, Three-Dimensional Ballistocardiography and respiratory motion in sustained microgravity, *Aviat. Space. Environ. Med.*, 2001; 72: 1067-1074.

[4] Migeotte P-F., Tank J., Pattyn N., Funtova I., Baevsky R.M., Neyt X., Prisk G.K., Three dimensional ballistocardiography: methodology and results from microgravity and dry immersion, Engineering in Medicine and Biology Society, IEEE-EMBC, Aug. 30 2011-Sept. 3 2011, 4271 – 4274.

[5] Franzblau, S.A., Best, W.R., Guillemin, V.Jr., Marbarger, J.P., 'Three Dimensional Vector Ballistocardiography, J. Lab. and Clin. Med. 36:824, 1950.

[6] Migeotte P-F., S. De Ridder, J. Tank, N. Pattyn, I. Funtova, R. Baevsky, X. Neyt, G.K. Prisk, Three dimensional ballisto- and seismo-cardiography: HIJ wave amplitudes are poorly correlated to maximal systolic force vector. IEEE-EMBC, Aug. 28 2012-Sept. 1 2012, 5046 – 5049.

[7] Migeotte, P.-F., Dominique, T., & Sa, R. C. Dynamics of blood pressure, pulse wave transit time and systolic time intervals during acute gravity changes induced by parabolic flight. J. gravit. Physiol., 9(1), P77–P78. 2002